

Low-temperature, solvent-free solid-state synthesis of single-crystalline titanium nitride nanorods with different aspect ratios

Upendra A. Joshi^a, Soo Hyun Chung^b, Jae Sung Lee^{a,*}

^aDepartment of Chemical Engineering and School of Environmental Science and Engineering, Pohang University of Science and Technology (POSTECH), San 31 Hyoja-dong, Pohang 790-784, Korea

^bKorea Institute of Energy Research, Daejeon, 305-343, Korea

Received 12 October 2004; received in revised form 21 December 2004; accepted 26 December 2004

Abstract

Titanium nitride nanorods have been successfully synthesized by low temperature solid-state metathesis of titanium (III) chloride and sodium azide without using any organic solvent. The conditions required for the synthesis of these nanorods have been optimized. It was found that the temperature and time of reaction had a significant effect on the product morphology. Thermal treatment at 360 °C, for 3 days gave the nanorods of the aspect ratio ~ 10 (i.e. diameter ~ 50 nm and length ~ 500 nm), whereas the thermal treatment at 400 °C for 3 days gave the nanorods of the aspect ratio ~ 50 (i.e. diameter ~ 50 nm and length $\sim 2\text{--}3$ μm). Scanning and transmission electron microscopies clearly showed the rod-type morphology. Further evidence for the phase purity and crystallinity of titanium nitride nanorods was given by X-ray diffraction, field emission high-resolution electron microscopy and X-ray photoelectron spectroscopy analyses.

© 2005 Elsevier Inc. All rights reserved.

Keywords: Titanium nitride nanorods; Solid-state metathesis; Refractory ceramics; Semiconductor; Solvent-free synthesis

1. Introduction

Titanium nitride is a technologically important material that has many applications such as hard coating for cutting tools [1], as a diffusion barrier for micro-electronic devices [2], as an optical coating [3] and as a gold-colored surface for jewelry [4], because of its excellent chemical stability, good wear resistance, high electrical conductivity and high melting point (2950 °C).

Conventionally, TiN powder has been made by gas–solid reactions of titanium (IV) chloride (TiCl₄) with ammonia and reactions of metal powders or metal hydride with nitrogen, a mixture of nitrogen and hydrogen or ammonia, at elevated temperatures [5,6].

Most of these reactions require a very high processing temperature above 1000 °C, which is difficult to control and results in grain growth, and agglomeration of the powder. Furthermore, low-energy chemical molecule precursor route, solid-state metathesis (SSM) routes, and solid–liquid metathesis route have been demonstrated for synthesis of TiN powders [7–10]. Material preparation methods have important effects on the structures and properties of materials. Recently, various solution chemical synthesis methods have been utilized to synthesize advanced nanostructure materials. These methods allow a good control over morphology of nanostructured materials [11,12]. Qian and co-workers [13,14] adopted a low-temperature benzene-thermal route for synthesis of nanocrystalline gallium nitride and titanium nitride particles with an average grain size of 50 nm. Hector et al. [8] prepared various transition

*Corresponding author. Fax: +82 54 279 5528.

E-mail address: jlee@postech.ac.kr (J.S. Lee).

metal nitrides by SSM. Considerable efforts also have been devoted to synthesize one dimensional nitride nanostructure materials that have potential technological importance such as GaN [15,16], BN [17], and AlN [18], etc. These materials of the low-dimension are known to have unique electronic, optical and mechanical properties [19,20].

In this communication, we report for the first time low-temperature, solvent-free synthesis of single crystalline TiN nanorods. Titanium nitride nanorods obtained by the metathesis reaction of sodium azide (NaN_3) and titanium (III) chloride (TiCl_3) in the autoclave at 360–400 °C under nitrogen atmosphere for 3 days without any solvent. As we do not use any solvent like benzene, contamination due to benzene carbonization is avoided. Furthermore, the dimensions of the nanorods could be tuned by simple variation of preparation conditions such as reaction temperature and time.

2. Experimental

Titanium (III) chloride (99.999%), sodium azide (99.99 + %) powders were obtained from Aldrich and used without any further purification. Titanium (III) chloride and sodium azide are highly corrosive and explosive materials therefore they should be handled very carefully. All the operations were carried out in a glove box filled with nitrogen in the absence of air or moisture (<5 ppm). In a typical synthesis, 3.08 g of titanium (III) chloride and 3.9 g of sodium azide were mixed together in a mortar pestle in absence of any solvent. The mixture is transferred into a Parr autoclave (300 cm³). An autoclave was then sealed and taken out of glove box, flushed and filled with nitrogen, heated electrically at 360–400 °C for 3 days without disturbing. It was then cooled down to room temperature and nitrogen pressure was released. The product was collected and washed several times with 0.1 M hydrochloric acid to remove the side product NaCl. Finally, brown–black powder was dried under vacuum at 70 °C for 12 h.

The product was characterized by powder X-ray diffraction (XRD MAC Science M18XHF diffractometer) using $\text{CuK}\alpha$ radiation ($\lambda = 1.5418 \text{ \AA}$). The morphology of nanostructures were determined by transmission electron microscopy (TEM, Philips CM-20) using an accelerating voltage of 200 kV and with field emission high resolution transmission electron microscopy (FE-HREM, Jeol 2100F). The field emission scanning electron microscopy (FE-SEM, FEI XL30S) analysis was carried out to see the overall morphology. The composition of TiN nanostructure was determined by X-ray photoelectron spectroscopy (XPS, VG Scientific ESCALAB 220iXL). The spectrometer was equipped with a hemi-spherical analyzer and all XPS

data presented here were acquired using $\text{MgK}\alpha$ X-ray (1253.6 eV). Sputter cleaning was done with a differentially pumped Ar^+ sputter gun. The nanorod compositions were estimated from the relative area intensities of different high-resolution peaks after normalizing with respective relative sensitivity factors in the software package. The as-obtained TiN nanorods were sputter etched in situ with Ar^+ to remove the oxide layer which is formed due to oxidation at room temperature.

CAUTION! These reactions are extremely exothermic and produce large quantities of nitrogen. A large reactor should be used to minimize the risk of pressure explosions.

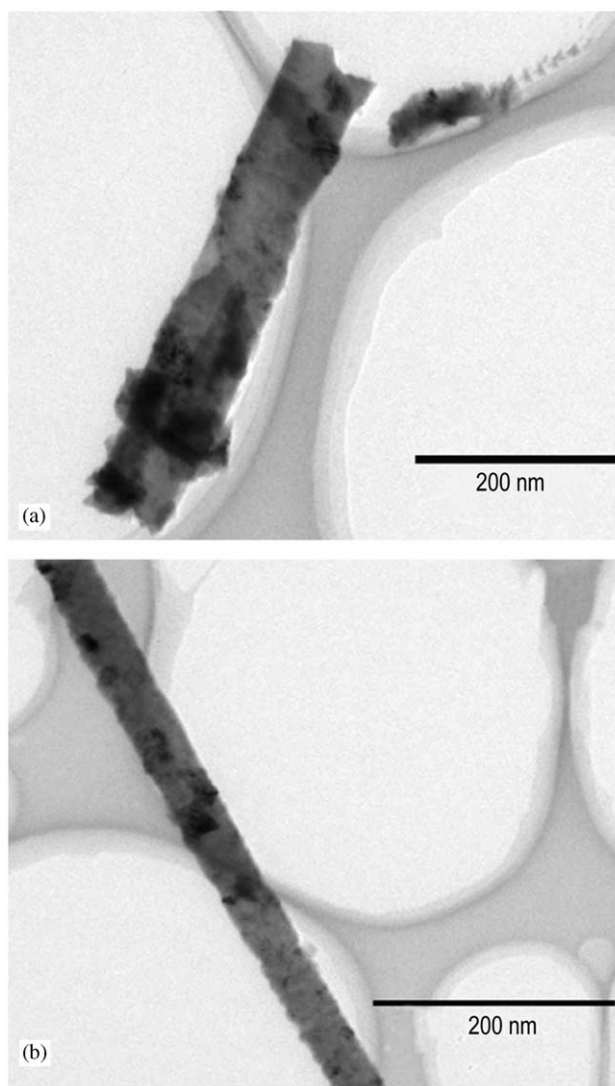


Fig. 1. TEM images of titanium nitride nanorods, (a) nanorods with the aspect ratio ~ 10 (diameter ~ 50 nm and length ~ 500 nm) obtained by thermal treatment at 360 °C for 3 days. (b) Nanorods with the aspect ratio ~ 50 (diameter ~ 50 nm and length $\sim 2\text{--}3 \mu\text{m}$) obtained by thermal treatment at 400 °C for 3 days.

3. Results and discussion

Representative transmission electronmicroscope (TEM) images of the titanium nitride nanorods are shown in Fig. 1. These images clearly reveal that the product is nanorods with diameter of ~ 50 nm and length of 2–3 μm (as in Fig. 1B). It was found that the product morphology depended upon synthesis conditions. The influence of reaction temperature on the formation of nanorods was investigated. Thermal treatment at 360 °C for 3 days gives the nanorods of the aspect ratio ~ 10 (i.e. diameter ~ 50 nm and length ~ 500 nm) as shown in Fig. 1A, whereas the thermal treatment at 400 °C for 3 days gives extended nanorods of the aspect ratio ~ 50 (i.e. diameter ~ 50 nm and length $\sim 2\text{--}3$ μm) as in Fig. 1B.

The length of nanorods could be varied further from few to tens of micrometer and it depended upon the time and temperature of synthesis reaction. Hence, one can even obtain nanowires with aspect ratios greater than 50 with the same reaction at 400 °C and for a longer time (say 4–5 days). Fig. 2 represents the X-ray diffraction pattern of as-obtained titanium nitride nanorods. The sharp peaks of the XRD pattern shows that the material is of high purity and almost single crystalline in nature. The unit cell parameter (cubic) for TiN nanorods has been determined to be $a = 4.24$ Å which is in good agreement with the literature value (JCPDS 38-1420).

Fig. 3 shows SEM images of as-prepared TiN nanorods. From Fig. 3A, it is evident that the TiN product mainly consists of straight and crystalline rod-like structures, with length ~ 500 nm – 1 μm and diameter ~ 50 nm. Fig. 3B shows the nanorods with aspect ratio ~ 50 , i.e. length $\sim 2\text{--}3$ μm and diameter ~ 50 nm. These results are consistent with those of TEM.

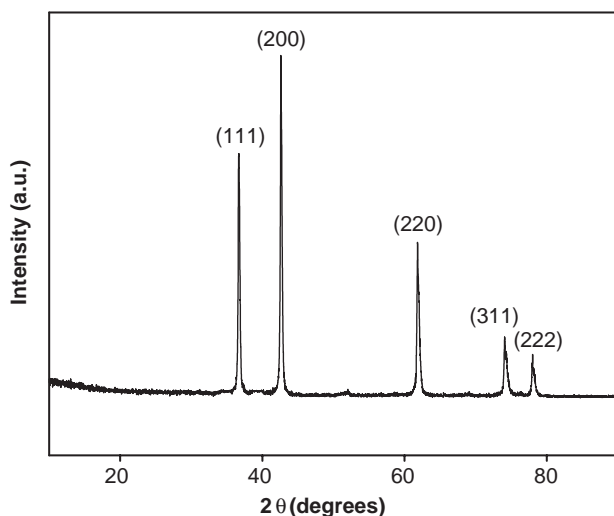


Fig. 2. X-ray diffraction pattern of titanium nitride nanorods obtained by the thermal treatment at 400 °C for 3 days. Sharp peaks show the phase purity and single-crystallinity of the titanium nitride nanorods.

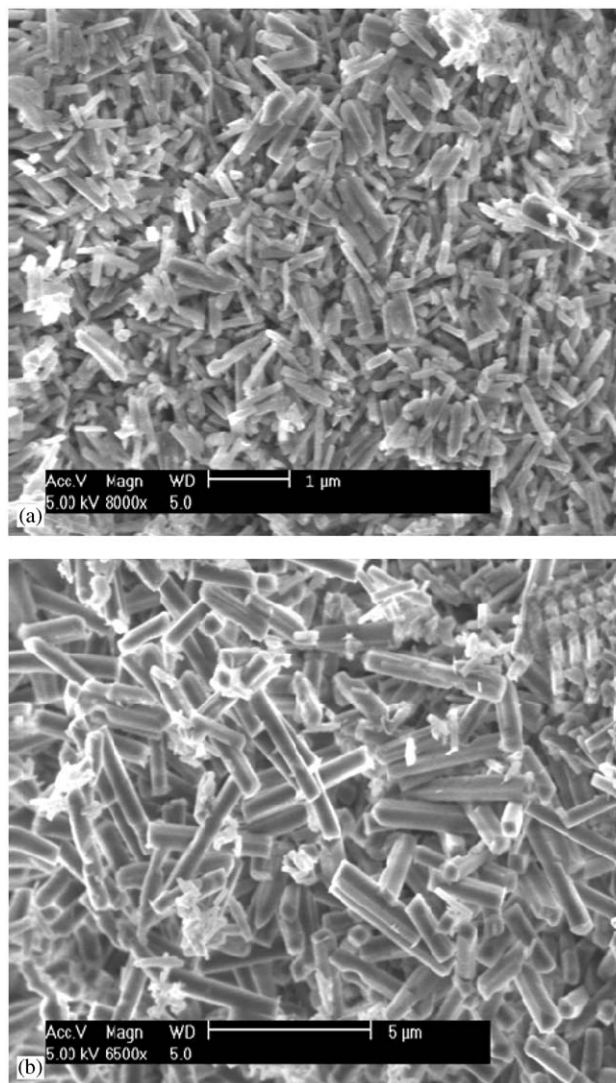


Fig. 3. Scanning Electron Microscopy (SEM) images of titanium nitride nanorods, (a) nanorods with the aspect ratio ~ 10 (diameter ~ 50 nm and length ~ 500 nm) obtained by thermal treatment at 360 °C for 3 days. (b) Nanorods with the aspect ratio ~ 50 (diameter ~ 50 nm and length $\sim 2\text{--}3$ μm) obtained by thermal treatment at 400 °C for 3 days.

Although there is some degree of aggregation and clumping the majority of nanorods exhibits well-defined individual morphologies.

Further evidence for the formation of single-crystalline titanium nitride nanorods could be found in HREM images shown in Fig. 4. These HREM images clearly show the tip of nanorod and the lattice fringes which are consistent throughout the crystal. The spacing between adjacent lattice planes is 0.21 nm, corresponding to (200) plane of NaCl type titanium nitride, which indicates that the preferred growth direction of nanorods is perpendicular to [200].

To investigate the electronic state of N and Ti in nanorods, we carried out the XPS analysis. Fig. 5 represents the XPS spectra of the titanium nitride

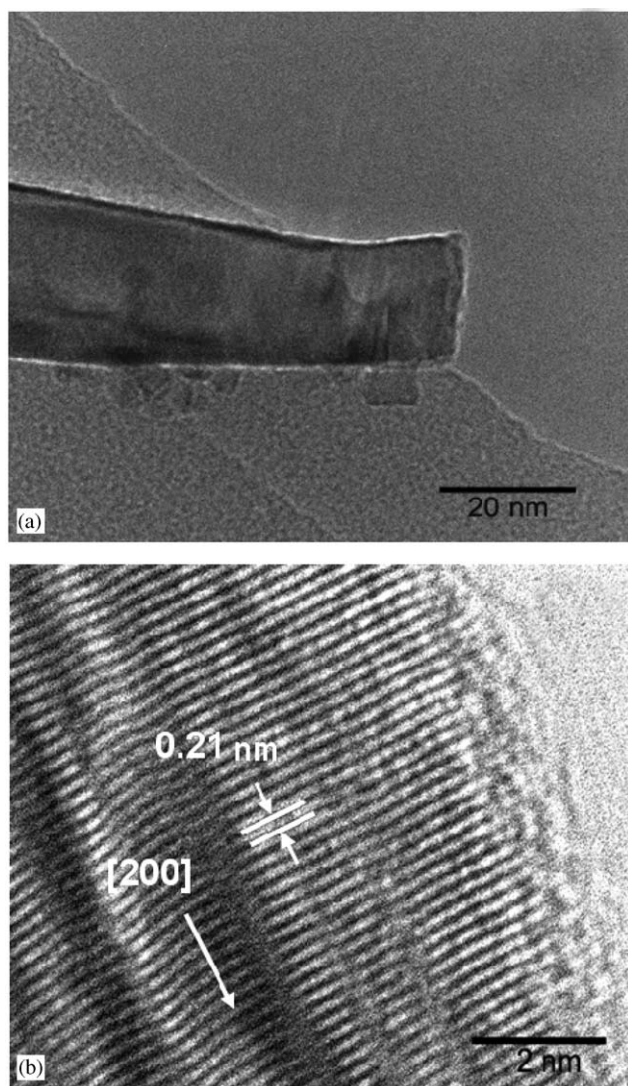


Fig. 4. Field emission high resolution electron microscopy (FE-HREM) images of titanium nitride nanorods, (a) a tip of a nanorod, and (b) lattice image that shows a spacing of 0.21 nm between adjacent lattice planes which corresponds to (200) plane of NaCl type titanium nitride. The preferential growth direction is perpendicular to [200].

nanorods. The binding energy of N 1s peak shown in Fig. 5A for titanium nitride nanorods matches very well with the literature value of 397.0 eV [21]. The broad shoulder toward high binding energies represents the presences of nitrogen species which is not directly associated with titanium. Similarly, the binding energies of Ti 2p doublet lines shown in Fig. 5B for TiN nanorods were determined to be 455 ± 0.2 eV and 461 ± 0.2 eV, which are in agreement with the published literature values for titanium nitride [21]. Furthermore, the quantification of peak areas gave the Ti:N atomic ratio 1:1. Hence we can conclude that our titanium nanorods are phase-pure and no TiO₂ impurity is present in the sample.

The synthesis of various refractory ceramics via SSM reaction has been reviewed by Gillan et al. [22]. The

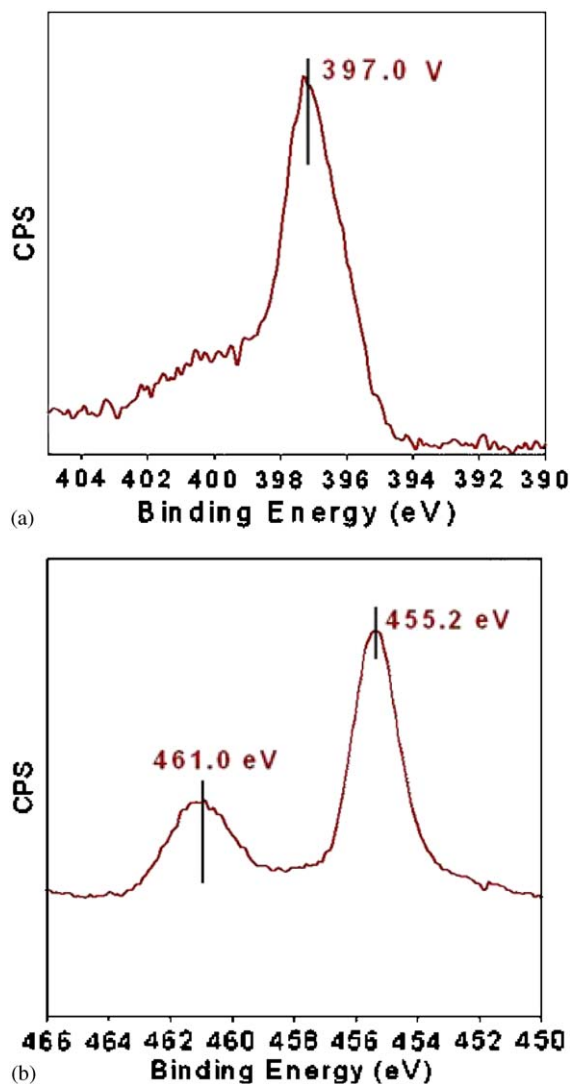
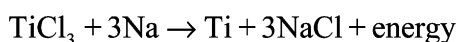
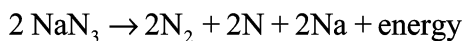


Fig. 5. An X-ray photoelectron spectrum of titanium nanorods. (A) N 1s spectra shows the peak at 397.0 eV. (B) Peaks at ~ 455 and ~ 461 eV of Ti 2p_{3/2} doublet matches with the literature values.

reaction between sodium azide and metal chlorides are exothermic as assessed by Hess' law. Although the reaction of TiCl₃ and NaN₃ to form TiN is thermodynamically spontaneous ($\Delta G_f^{\circ} = -354.7$ kcal/mol) [23], it is well known that the TiN could not be obtained at a temperature < 330 °C (thermal decomposition temperature of reactant) [22–24]. Hence we investigated the whole process to find the optimum condition for the formation of nanorods as described above.

The thermal decomposition of NaN₃ proceeds according to the equation, $2\text{NaN}_3 \rightarrow 3\text{N}_2 + 2\text{Na}$. A previous report on the details of the reaction indicates that nitrogen atoms can be generated from this decomposition process [25]. Adopting the same idea, another report [13] proposed a reaction mechanism that could be represented as Scheme 1, in the synthesis of



Scheme 1. Formation mechanism of titanium nitride.

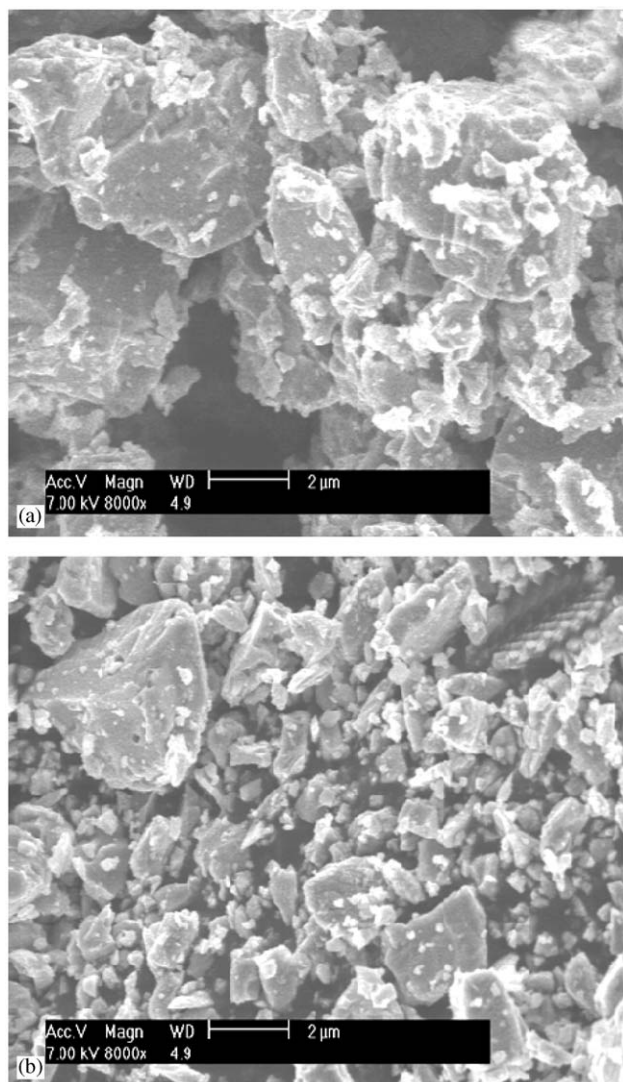


Fig. 6. SEM images of TiN powder (A) before heating with NaCl salt, and (B) after heating with NaCl salt at 360 °C, 600 psi N₂ pressure for 3 days.

spherical titanium nitride nanocrystals in benzene solvothermal process. We presume essentially the same mechanism could dictate the formation of titanium nitride nanorods discussed in the present study.

The reason for the formation of nanorods is not understood at the moment. Yamane and co-workers reported the GaN crystal growth in molten Na-flux [26,27]. They obtained GaN prisms and platelets in the range of 0.2–1 mm size. Likewise, one can consider the

possibility of TiN crystal growth in molten Na formed in the first step of the Scheme 1. However, it is expected that formed Na is consumed immediately by the facile second reaction to form NaCl byproduct. NaCl would be in solid state under the synthesis conditions and would not contribute to the crystal growth of TiN. Indeed, when we heated a commercial TiN powder (Aldrich) with a morphology shown in Fig. 6A together with NaCl (TiN : NaCl = 1:1 in moles) under the same reaction condition (360 °C, 600 psi, for 3 days), we could not find any nanorods formed in this process as shown Fig. 6B.

Since TiN has a cubic structure, there is no intrinsic preferred orientation of crystal growth. Increase in aspect ratio (maintaining the same diameter) with synthesis time and temperature suggests that a kinetic factor might be responsible for the unidirectional growth. Thus, after the formation of nanocrystals, they may grow in one direction as we provide more time maintaining the constant temperature and pressure conditions. In presence of solvent like benzene, solvothermal synthesis yielded nanocrystalline TiN particles of spherical shape as reported earlier [13]. Thus, solvent may exert an important influence on the geometry of the obtained product as also demonstrated in the synthesis of alumina nanotubes [28]. In any case, as we do not use any solvent like benzene, contamination due to benzene carbonization is avoided.

4. Conclusions

Single-crystalline titanium nitride nanorods have been successfully synthesized by low temperature SSM of titanium (III) chloride and sodium azide without using any organic solvent. The synthesis temperature and time could be varied for the synthesis of TiN nanorods with different aspect ratios. The SEM and TEM images clearly show the rod type morphology. Further evidence for the phase purity and crystallinity of titanium nitride nanorods was given by an X-ray diffraction, FE-TEM images and an X-ray photoelectron spectroscopy analysis. The present method allows the fabrication of single-crystalline TiN nanorods with tunable dimensions under mild conditions.

Acknowledgment

This work has been supported by National Research and Development project for Nanoscience and Technology, Hydrogen R&D center, and the Research Center for Energy Conversion and Storage. We appreciate the support of the Korea Ministry of Education and Human Resources Development through the BK 21 program.

Reference

- [1] R. Bühl, H.K. Pulker, E. Moll, *Thin Solid Films* 80 (1981) 265–270.
- [2] G.I. Grigorov, K.G. Grigorov, M. Stoyanova, J.L. Vignes, J.P. Langeron, P. Denjean, *Appl. Phys. A* 57 (1993) 195–197.
- [3] E. Velkonen, T. Karlsson, B. Karlsson, B.O. Johansson, *Proc. SPIE 1983 Int. Conf.* 401 (1983) 41.
- [4] B. Zega, M. Kornmann, J. Amiguet, *Thin Solid Films* 45 (1977) 577–582.
- [5] L. Toth, *Transition Metal Carbides and Nitrides*, Academic Press, New York, 1971, p. 176.
- [6] C.C. Addison, B.M. Davies, *J. Chem. Soc. A* (1969) 1822–1827.
- [7] A. Hector, I.P. Parkin, *J. Chem. Soc. Chem. Commun.* (1993) 1095–1096.
- [8] A.L. Hector, I.P. Parkin, *Polyhedron* 14 (1995) 913–917.
- [9] E.G. Gillan, R.B. Kaner, *Inorg. Chem.* 33 (1994) 5693–5700.
- [10] I.P. Parkin, *Chem. Soc. Rev.* (1996) 199–207.
- [11] Y. Xia, P. Yang, Y. Sun, Y. Wu, B. Mayers, B. Gates, Y. Yin, F. Kim, H. Yan, *Adv. Mater.* 15 (2003) 353–389.
- [12] J. Hu, T.W. Odom, C.M. Lieber, *Acc. Chem. Res.* 32 (1999) 435–445.
- [13] J. Hu, Q. Lu, K. Tang, S. Yu, Y. Qian, G. Zhou, X. Liu, *J. Am. Ceram. Soc.* 83 (2000) 430–432.
- [14] Y. Xie, Y. Qian, W. Wang, S. Zhang, Y. Zhang, *Science* 272 (1996) 1926–1927.
- [15] W. Han, S. Fan, Q. Li, Y. Hu, *Science* 277 (1997) 1287–1289.
- [16] J. Goldberger, R. He, Y. Zhang, S. Lee, H. Yan, H.J. Choi, P. Yang, *Nature* 422 (2003) 599–602.
- [17] N.G. Chopra, R.J. Luyken, K. Cherrey, V.H. Crespi, M.L. Cohen, S.G. Louie, A. Zettl, *Science* 269 (1995) 966–968.
- [18] Q. Wu, Z. Hu, X. Wang, Y. Lu, X. Chen, H. Xu, Y. Chen, *J. Am. Chem. Soc.* 125 (2003) 10176–10177.
- [19] Y. Hung, X. Duan, Y. Cui, C.M. Lieber, *Nano Lett.* 2 (2002) 101–104.
- [20] J.-R. Kim, et al., *Appl. Phys. Lett.* 80 (2002) 3548–3550.
- [21] N.C. Saha, H.G. Tompkins, *J. Appl. Phys.* 72 (1992) 3072–3079.
- [22] E.G. Gillan, R.B. Kaner, *Chem. Mater.* 8 (1996) 333–343.
- [23] R.C. Weast (Ed.), *Handbook of Chemistry and Physics*, CRC Press, Boca Raton FL, 1987.
- [24] E.A. Secco, *Canad. J. Chem.* 40 (1962) 2191–2194.
- [25] G.D. Singer, H.J. Mueller, *Nature* 207 (1965) 1073–1075.
- [26] H. Yamane, M. Shimada, T. Sekiguchi, F.J. DiSalvo, *J. Cryst. Growth* 186 (1998) 8–12.
- [27] M. Aoki, H. Yamane, M. Shimada, T. Kajiwara, S. Sarayama, F.J. DiSalvo, *Cryst. Growth Design* 2 (2002) 55–58.
- [28] H.C. Lee, H.J. Kim, S.H. Chung, K.H. Lee, J.S. Lee, *J. Am. Chem. Soc.* 125 (2003) 2882–2883.